

LETTER TO THE EDITOR

# The IRAM-30m line survey of the Horsehead PDR: I. $\text{CF}^+$ as a tracer of $\text{C}^+$ and a measure of the Fluorine abundance

V. Guzmán<sup>1</sup>, J. Pety<sup>1,2</sup>, P. Gratier<sup>1</sup>, J.R. Goicoechea<sup>3</sup>, M. Gerin<sup>2</sup>, E. Roueff<sup>4</sup>, and D. Teyssier<sup>5</sup>

<sup>1</sup> IRAM, 300 rue de la Piscine, 38406 Saint Martin d'Hères, France  
e-mail: [guzman;pety;gratier]@iram.fr

<sup>2</sup> LERMA - LRA, UMR 8112, Observatoire de Paris and Ecole normale Supérieure, 24 rue Lhomond, 75231 Paris, France.  
e-mail: maryvonne.gerin@lra.ens.fr

<sup>3</sup> Centro de Astrobiología. CSIC-INTA. Carretera de Ajalvir, Km 4. Torrejón de Ardoz, 28850 Madrid, Spain.  
e-mail: jr.goicoechea@cab.inta-csic.es

<sup>4</sup> LUTH UMR 8102, CNRS and Observatoire de Paris, Place J. Janssen, 92195 Meudon Cedex, France.  
e-mail: evelyne.roueff@obspm.fr

<sup>5</sup> European Space Astronomy Centre, ESA, PO Box 78, 28691 Villanueva de la Caada, Madrid, Spain  
e-mail: dteyssier@sciops.esa.int

Preprint online version: January 28, 2018

## ABSTRACT

$\text{C}^+$  is a key species in the interstellar medium but its  $158 \mu\text{m}$  fine structure line cannot be observed from ground-based telescopes. Current models of fluorine chemistry predict that  $\text{CF}^+$  is the second most important fluorine reservoir, in regions where  $\text{C}^+$  is abundant. We detected the  $J = 1 - 0$  and  $J = 2 - 1$  rotational lines of  $\text{CF}^+$  with high signal-to-noise ratio towards the PDR and dense core positions in the Horsehead. Using a rotational diagram analysis, we derive a column density of  $N(\text{CF}^+) = (1.5 - 2.0) \times 10^{12} \text{ cm}^{-2}$ . Because of the simple fluorine chemistry, the  $\text{CF}^+$  column density is proportional to the fluorine abundance. We thus infer the fluorine gas-phase abundance to be  $F/H = (0.6 - 1.5) \times 10^{-8}$ . Photochemical models indicate that  $\text{CF}^+$  is found in the layers where  $\text{C}^+$  is abundant. The emission arises in the UV illuminated skin of the nebula, tracing the outermost cloud layers. Indeed,  $\text{CF}^+$  and  $\text{C}^+$  are the only species observed to date in the Horsehead with a double peaked line profile caused by kinematics. We therefore propose that  $\text{CF}^+$ , which is detectable from the ground, can be used as a proxy of the  $\text{C}^+$  layers.

**Key words.** Astrochemistry – ISM: clouds – ISM: molecules – ISM: individual objects: Horsehead nebula – Radio lines: ISM

## 1. Introduction

$\text{C}^+$  is a key species in the interstellar medium. First, it is an important tracer of the neutral gas where CO has not been able to form yet (Langer et al. 2010). Second, it is the dominant gas phase reservoir of carbon in the diffuse interstellar medium and its fine structure transition ( $^2P_{3/2} - ^2P_{1/2}$   $157.8 \mu\text{m}$ ,  $1.9 \text{ THz}$ ) is the major cooling mechanism of the diffuse gas. Unfortunately, its rest-frame emission cannot be observed from ground-based telescopes. With Herschel and SOFIA it is now possible to observe this line from space and from the stratosphere respectively, but with limited spatial resolution ( $12''$  and  $15''$ , respectively). It is therefore of great interest to find tracers of  $\text{C}^+$  that can be observed from the ground at much higher spatial resolution, for example with the Atacama Large Millimeter Array (ALMA) or the Northern Extended Millimeter Array (NOEMA).

The chemistry of fluorine was studied by Neufeld et al. (2005). Although there are still uncertainties in some reaction rate coefficients (e.g.  $\text{CF}^+$  photodissociation), the current models predict that  $\text{CF}^+$  is present in regions where  $\text{C}^+$  and HF are abundant, as it is produced by reactions between these species and destroyed mainly by electrons. In these regions  $\text{CF}^+$  is the second most important fluorine reservoir, after HF. The ground rotational transition of HF, which lies at THz frequencies, was first detected with the HIFI/Herschel in the diffuse interstellar medium through absorption measurements (Neufeld et al. 2010) and in emission in the Orion Bar (van der Tak et al. 2012).

Neufeld et al. (2010) find a lower limit for the HF abundance of  $6 \times 10^{-9}$  relative to hydrogen nuclei, providing support to the theoretical prediction that HF is the dominant fluorine reservoir under a wide variety of interstellar conditions. Unlike HF and  $\text{C}^+$ ,  $\text{CF}^+$  rotational lines can be observed from the ground. However, up to now there has been only one detection of  $\text{CF}^+$  towards the Orion Bar (Neufeld et al. 2006).

In this letter we report the detection of  $\text{CF}^+$  at the HCO and  $\text{DCO}^+$  peak emission, corresponding respectively to the PDR and dense core environments in the Horsehead nebula (Pety et al. 2007; Gerin et al. 2009). We then infer the gas phase fluorine abundance.

## 2. Observations and data reduction

Fig. 1 displays deep integrations of the  $J = 1 - 0$  and  $J = 2 - 1$  low-energy rotational lines of  $\text{CF}^+$  with the IRAM-30m telescope centered at the PDR and the dense core, located respectively at  $(\delta\text{RA}, \delta\text{DEC}) = (-5'', 0'')$  and  $(20'', 22'')$  with respect to the projection center, with  $49 \text{ kHz}$  spectral resolution at both frequencies. These observations were obtained as part of the Horsehead WHISPER project (Wideband High-resolution Iram-30m Surveys at two Positions with Emir Receivers). A presentation of the whole survey and the data reduction process will be given in Pety et al. 2012, in prep.

The  $\text{CF}^+$   $J = 1 - 0$  and  $J = 2 - 1$  maps displayed in Fig. 2 were observed simultaneously during 7 hours of good winter

Table 1: Observation parameters for the maps. Their projection center is  $\alpha_{2000} = 05^h40^m54.27^s$ ,  $\delta_{2000} = -02^\circ28'00''$ .

Line	Frequency GHz	Instrument	$F_{\text{eff}}$	$B_{\text{eff}}$	Beam arcsec	PA °	Int. Time <sup>a</sup> hours	$T_{\text{sys}}$ K ( $T_{\text{A}}^*$ )	Noise K ( $T_{\text{mb}}$ )	Obs.date
HCO $1_{0,1} 3/2, 2 - 0_{0,0} 1/2, 1$	86.670760	PdBI/C&D	0.95	0.78	$6.7 \times 4.4$	16	6.5	150	0.09	2006-2007
CF <sup>+</sup> $1 - 0$	102.587533	30m/EMIR	0.94	0.79	25.4	0	2.5	88	0.03 <sup>b</sup>	Jan. 2012
CF <sup>+</sup> $2 - 1$	205.170520	30m/EMIR	0.94	0.64	11.4	0	3.4	220	0.18 <sup>c</sup>	Jan. 2012
DCO <sup>+</sup> $3 - 2$	216.112582	30m/HERA	0.90	0.52	11.4	0	1.5	230	0.10	Mar. 2006

<sup>a</sup> On-source integration time. The noise values are for a spectral resolution of <sup>b</sup> 0.114 km s<sup>-1</sup> and <sup>c</sup> 0.057 km s<sup>-1</sup>.

weather (2mm of precipitable water vapor) using the EMIR sideband-separation receivers at the IRAM-30m. We used the position-switching, on-the-fly observing mode. The off-position offsets were  $(\delta\text{RA}, \delta\text{Dec}) = (-100'', 0'')$ , i.e. into the HII region ionized by  $\sigma\text{Ori}$  and free of molecular emission. We observed along and perpendicular to the direction of the exciting star in zigzags, covering an area of  $100'' \times 100''$ . A description of the HCO and DCO<sup>+</sup> observations and data reductions, which are also displayed in Fig. 2, can be found in Gerin et al. (2009) and Pety et al. (2007). Table 1 summarizes the observation parameters for all these maps.

The maps were processed with the GILDAS<sup>1</sup> softwares (Pety 2005). The IRAM-30m data were first calibrated to the  $T_{\text{A}}^*$  scale using the chopper-wheel method (Penzias & Burrus 1973), and finally converted to main-beam temperatures ( $T_{\text{mb}}$ ) using the forward and main-beam efficiencies ( $F_{\text{eff}}$  &  $B_{\text{eff}}$ ) displayed in Table 1. The resulting amplitude accuracy is  $\sim 10\%$ . The resulting spectra were then baseline-corrected and gridded through convolution with a Gaussian to obtain the maps.

### 3. Results

#### 3.1. Line profiles

Two velocity peaks for the  $J = 1 - 0$  line are clearly seen at both positions in Fig. 1. The second velocity peak is marginal for the  $J = 2 - 1$  line. Table 2 presents the results of dual Gaussian fits. The centroid velocity of each peak is significantly shifted between the two CF<sup>+</sup> transitions. We have carefully checked that neither peak is a residual line incompletely rejected from the image side band. This doubled-peak behavior is unexpected because all species without an hyperfine structure detected previously at millimeter wavelengths in the Horsehead present a simple velocity profile centered close to 10.7 km s<sup>-1</sup>. The only other species detected to date with a clear double peak emission profile is C<sup>+</sup> towards the illuminated edge of the cloud (HIFI/Herschel, Teyssier et al. 2012 in prep).

The most obvious explanation would be that the higher velocity peak corresponds to another line from another species. However, there are no other lines in the public line catalogs (Pickett et al. 1998; Müller et al. 2001) near this frequency besides CF<sup>+</sup>. Another possible explanation would be that the two peaks correspond to different hyperfine components which are caused by the fluorine nuclei. To our knowledge, there are no hyperfine structure studies on CF<sup>+</sup>. However, as the molecule is isoelectronic with CO, one can try to rely on <sup>13</sup>CO spectroscopy since the nuclear spin of <sup>13</sup>C is 1/2, as for the fluorine nucleus. The magnetic dipolar coupling constant scales approximately with the rotational constant and the magnetic moment of the nucleus for <sup>1</sup> $\Sigma$  electronic ground states (Reid & Chu 1974). This allows us to derive a coupling constant of approximately

<sup>1</sup> See <http://www.iram.fr/IRAMFR/GILDAS> for more information about the GILDAS softwares.

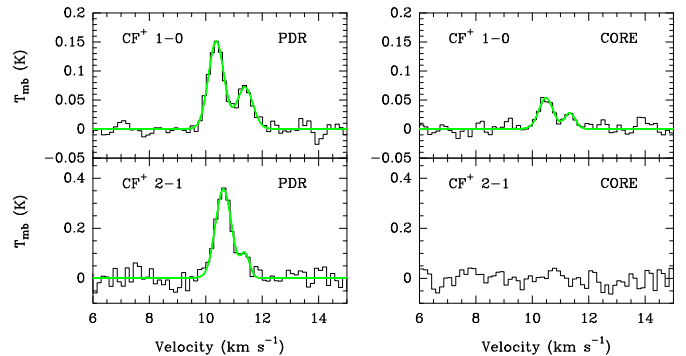


Fig. 1: Deep integrations towards the PDR and core positions. The green lines are double gaussian fits.

110 kHz, and an hyperfine splitting of 165 kHz (110 kHz) for the  $J = 1 - 0$  ( $J = 2 - 1$ ) transitions, well below the observations. In addition, the respective intensities do not follow the theoretical predictions. Therefore, this possibility is unlikely. The profile is not caused by self-absorption because the CF<sup>+</sup> opacities are low ( $\tau \lesssim 1$ ). We thus attribute the complex line profiles to kinematics in the CF<sup>+</sup> emitting layers.

#### 3.2. CF<sup>+</sup> spatial distribution

Fig. 2 presents the CF<sup>+</sup>, HCO and DCO<sup>+</sup> integrated line intensity maps. The CF<sup>+</sup> emission is concentrated towards the edge of the Horsehead, delineating the western edge of the DCO<sup>+</sup> emission. A more extended and fainter emission is detected in the CF<sup>+</sup>  $J = 1 - 0$  map but not in the  $J = 2 - 1$  map, which has a lower signal-to-noise ratio. The intensity peak of the CF<sup>+</sup>  $J = 1 - 0$  line coincides with the intensity peak of the HCO emission (shown by the green cross), which traces the far UV illuminated matter (Gerin et al. 2009). The  $J = 2 - 1$  transition also peaks near the HCO emission peak.

Table 2: Gaussian fit results.

Line	Line area K km s <sup>-1</sup>	Velocity km s <sup>-1</sup>	Width km s <sup>-1</sup>	$T_{\text{peak}}$ K
PDR				
CF <sup>+</sup> $J = 1 - 0$	0.10±0.01	10.36±0.02	0.65±0.04	0.15
	0.05±0.01	11.38±0.03	0.66±0.09	0.07
CF <sup>+</sup> $J = 2 - 1$	0.25±0.02	10.62±0.02	0.67±0.06	0.36
	0.04±0.02	11.39±0.06	0.38±0.17	0.09
CORE				
CF <sup>+</sup> $J = 1 - 0$	0.03±0.01	10.47±0.04	0.60±0.08	0.05
	0.01±0.01	11.32±0.06	0.45±0.20	0.03
CF <sup>+</sup> $J = 2 - 1$	< 0.05 <sup>a</sup>	10.7 <sup>a</sup>	0.5 <sup>a</sup>	0.09 <sup>a</sup>

<sup>a</sup> Upper limit for a fixed velocity, linewidth and a  $T_{\text{peak}} = 2\sigma_{\text{RMS}}$

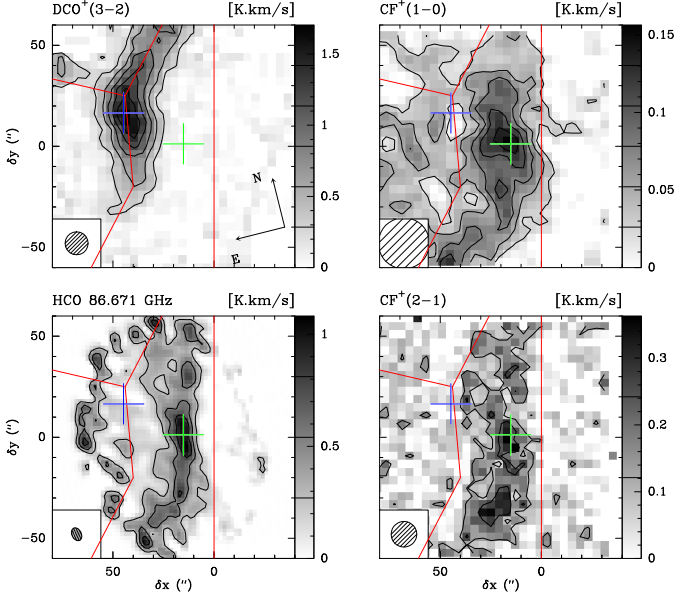


Fig. 2: Integrated intensity maps of the Horsehead edge. Maps were rotated by 14° counter-clockwise around the projection center, located at  $(\delta x, \delta y) = (20'', 0'')$ , to bring the exciting star direction in the horizontal direction and the horizontal zero was set at the PDR edge, delineated by the red vertical line. The crosses show the positions of the PDR (green) and the dense core (blue). The spatial resolution is plotted in the bottom left corner. Values of the contour levels are shown on the color look-up table of each image (first contour at  $2\sigma$  and  $2.5\sigma$  for CF<sup>+</sup> 1–0 and 2–1 respectively). The emission of all lines is integrated between 10.1 and 11.1 km s<sup>-1</sup>.

We have checked that beam pick-up contamination from the PDR is negligible at the core position ( $< 7\%$ ), even with the large beam size ( $\sim 25''$ ) of the 30m at 102 GHz. The emission then arises in the line of sight towards the core but not necessarily in the cold gas associated with the core. Indeed, we expect the CF<sup>+</sup> emission to arise in the outer layers of the nebula, delineating the edge as shown by the maps. This emission is likely to arise in the warmer and more diffuse material of the skin layers towards the core line of sight. Furthermore, there is a minimum of the emission in the CF<sup>+</sup> 1–0 map towards the dense core position. This confirms that the CF<sup>+</sup> emission is associated to the diffuse envelope. Molecular emission from the lower density cloud surface was already mentioned by Goicoechea et al. (2006) and Gerin et al. (2009) to explain the CS and HCO emission, respectively.

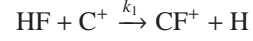
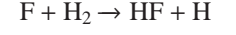
### 3.3. Column densities and abundances

The CF<sup>+</sup> column density is estimated assuming that the emission is optically thin and that the emission fills the 30m beam. We infer an excitation temperature of 10 K, based on a rotational diagram built with the integrated line intensities of the two detected transitions. Assuming  $T_{\text{ex}} = 10$  K for all rotational levels, the beam averaged column density is  $\approx (1.5 - 2.0) \times 10^{12}$  cm<sup>-2</sup> in the PDR. This value is similar to the column density found in the Orion Bar by Neufeld et al. (2006). In the next section, we will show that the CF<sup>+</sup> emission arises at the illuminated edge of the nebula. Goicoechea et al. (2009a) found that the [O I] 63 μm fine structure line, which also arises at the edge of the nebula, was best reproduced with a gas density of  $n_{\text{H}} \approx 10^4$  cm<sup>-3</sup>. Thus, assuming this density and a cloud depth  $l \sim 0.1$  pc (Habart et al. 2005), the CF<sup>+</sup> column density translates into an abundance of

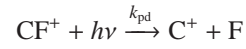
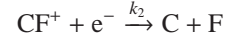
$\approx (4.9 - 6.5) \times 10^{-10}$  with respect to H nuclei. Taking the same excitation temperature of 10 K, we computed a column density towards the core of  $\approx 4.4 \times 10^{11}$  cm<sup>-2</sup>. We consider this as an upper limit for the model in Sect. 3.4 because CF<sup>+</sup> is found in the surface layer which is not taken into account by our unidimensional photochemical model.

### 3.4. CF<sup>+</sup> chemistry

CF<sup>+</sup> is formed through the following chemical path:



and destroyed by dissociative recombination with electrons (Neufeld et al. 2006) and by far UV photons:



The reactions rates are  $k_1 = 7.2 \times 10^{-9} (T/300)^{-0.15}$  cm<sup>3</sup> s<sup>-1</sup> (Neufeld et al. 2005) and  $k_2 = 5.3 \times 10^{-8} (T/300)^{-0.8}$  cm<sup>3</sup> s<sup>-1</sup> (Novotny et al. 2005). The CF<sup>+</sup> photodissociation rate  $k_{\text{pd}}$  is not known. Nevertheless, assuming a rate of  $10^{-9} \exp(-2.5 A_V)$  s<sup>-1</sup>, we estimate that this contribution is negligible compared to the dissociative recombination in low far UV field PDRs like the Horsehead. However, it might not be negligible in regions with high radiation fields ( $\chi \approx 10^4 - 10^5$ ), like the Orion Bar. In the following we thus assume that  $k_{\text{pd}} = 0$ . Because 1) the fluorine chemistry is simple, 2) the electron abundance is given by the ionization of carbon  $n(\text{e}^-) \sim n(\text{C}^+)$  and 3) HF is the major reservoir of fluorine  $n(\text{HF}) \sim n(\text{F})$ , it can be shown that the CF<sup>+</sup> column density is proportional to the fluorine gas phase abundance ( $[\text{F}] = \text{F}/\text{H}$ ), *i.e.*

$$N(\text{CF}^+) \approx \frac{k_1}{k_2} [\text{F}] n_{\text{H}} l \quad [\text{cm}^{-2}]$$

From our CF<sup>+</sup> observations we find  $\text{F}/\text{H} \approx (0.6 - 1.5) \times 10^{-8}$  in the Horsehead PDR (see Fig. 3), in good agreement with the solar value ( $2.6 \times 10^{-8}$ ; Asplund et al. 2009) and the one found in the diffuse atomic gas ( $1.8 \times 10^{-8}$ ; Snow et al. 2007). Sonnentrucker et al. (2010) also derived  $\text{F}/\text{H} \approx (0.5 - 0.8) \times 10^{-8}$  in diffuse molecular clouds detected in absorption with the HIFI/Herschel.

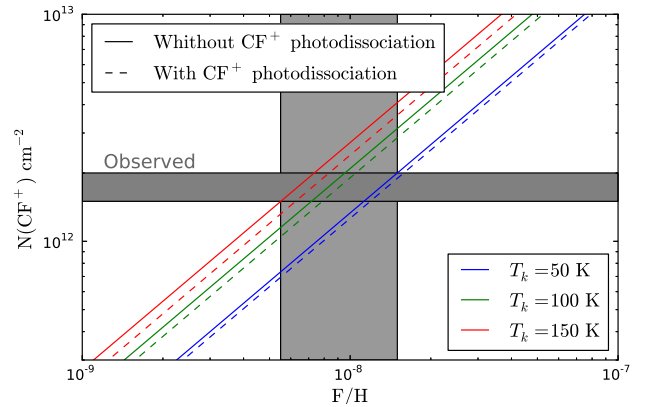


Fig. 3: Relation between the CF<sup>+</sup> column density and F/H.



In order to understand the CF<sup>+</sup> abundance profile as a function of depth, we used a one-dimensional, steady-state photochemical model (Meudon PDR code, Le Boulrot et al. 2012; Le Petit et al. 2006). The used version of the Meudon PDR model includes the Langmuir Hinshelwood and Eley-Rideal mechanisms to describe the formation of H<sub>2</sub> on grain surfaces. The physical conditions in the Horsehead have already been constrained by our previous observational studies and we keep the same assumptions for the steep density gradient (displayed in the upper panel of Fig. 4), radiation field ( $\chi = 60$  times the Draine (1978) mean interstellar radiation field), elemental gas-phase abundances (see Table 6 in Goicoechea et al. 2009b) and cosmic ray primary ionization rate ( $\zeta = 5 \times 10^{-17}$  s<sup>-1</sup> per H<sub>2</sub> molecule). We used the Ohio State University (osu) pure gas-phase chemical network, and included fluorine adsorption and desorption on grains.

The predicted CF<sup>+</sup>, HF and C<sup>+</sup> abundance profiles are shown in Fig. 4 (b). HF and CF<sup>+</sup> abundances decreases rapidly for  $A_V > 1$ . The model is in good agreement with the observed CF<sup>+</sup> abundance in the PDR, shown by the horizontal bars. The model predicts that there is a significant overlap between CF<sup>+</sup> and C<sup>+</sup>. Moreover, the abundance ratio between these two species remains quite constant along the illuminated side of the cloud, *i.e.*  $A_V < 4$ , as shown in Fig. 4 (c). The CF<sup>+</sup> emission arises in the outermost layers of the cloud ( $A_V \sim 0.5$ ), which are directly exposed to the far UV field and where the gas is less dense. The predicted spatial distribution of the CF<sup>+</sup> emission is shown in Fig. 4 (d). We expect a narrow filament ( $\sim 5''$ ) shifted in the illuminated part of the PDR with respect to the HCO emission, which has already shown to trace the far UV illuminated molecular gas (Gerin et al. 2009).

#### 4. Conclusions

We have detected the  $J = 1 - 0$  and  $J = 2 - 1$  rotational lines of CF<sup>+</sup> with high signal-to-noise ratio towards the PDR and core positions in the Horsehead. We have also mapped the region, and find that the emission arises mostly at the illuminated edge of the nebula (PDR), but it is also detected towards the dense core arising from its lower density skin. CF<sup>+</sup> is unique as its column density is proportional to the elemental abundance of fluorine. In the Horsehead PDR we find  $N \simeq (1.5 - 2.0) \times 10^{12}$  cm<sup>-2</sup> and infer F/H  $\simeq (0.6 - 1.5) \times 10^{-8}$ . Our model of the fluorine chemistry predicts that CF<sup>+</sup> accounts for 4-8% of all fluorine. CF<sup>+</sup> is found in the layers where C<sup>+</sup> is abundant as it is formed by reactions between HF and C<sup>+</sup>. In these regions the ionization fraction is high (see Goicoechea et al. 2009b) and CF<sup>+</sup> destruction is dominated by dissociative recombination with electrons. The CF<sup>+</sup> emission has two velocity components. The possibility that we are resolving the hyperfine structure is unlikely but corresponding theoretical or experimental study would allow to derive the velocity structure unambiguously. Although the CF<sup>+</sup> line profile is not exactly the same as the C<sup>+</sup> line profile, they are the only species in the Horsehead with a double-peaked profile of kinematic origin measured to date. The complex line profile of both CF<sup>+</sup> and C<sup>+</sup> therefore confirms that they trace the gas directly exposed to the far UV radiation, which shows a completely different kinematics than the following layers traced by other species, like HCO. We therefore propose that CF<sup>+</sup> can be used as a proxy of the C<sup>+</sup> layers which can be observed from the ground. We will check this by comparing with a HIFI/Herschel map of the C<sup>+</sup> emission in the Horsehead.

*Acknowledgements.* We thank the editor and anonymous referee for their useful comments that improved the letter. VG thanks support from the Chilean

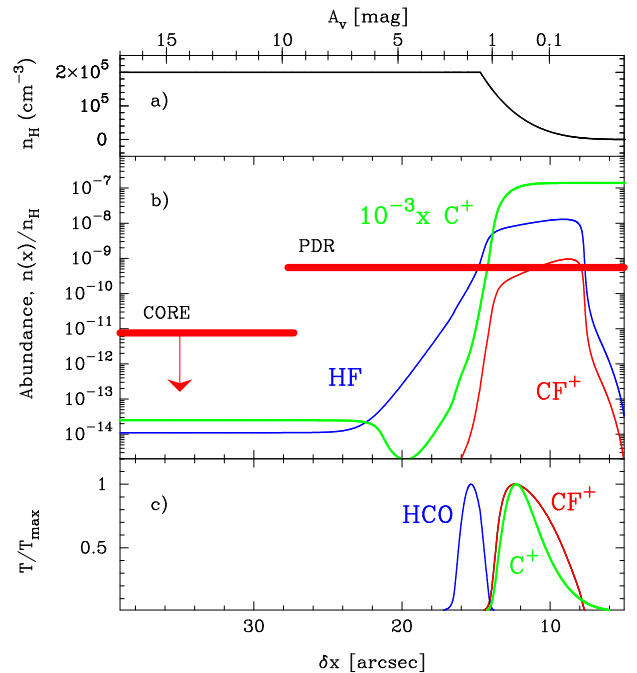


Fig. 4: Photochemical model of the Horsehead PDR.  $A_V$  increases from right to left and the PDR edge, delineated by the red vertical line in Fig. 2, corresponds to  $A_V = 0$ . a) Horsehead density profile  $n_H = n(\text{H}) + 2n(\text{H}_2)$ . b) Predicted abundance of CF<sup>+</sup> in red, HF in blue and C<sup>+</sup> in green. The red horizontal bars show the measured CF<sup>+</sup> abundances, and their length represents the beam size. c) Predicted intensity profiles.

Government through the Becas Chile scholarship program. This work was also funded by grant ANR-09-BLAN-0231-01 from the French *Agence Nationale de la Recherche* as part of the SCHISM project. JRG thanks the Spanish MICINN for funding support through grants AYA2009-07304 and CSD2009-00038. JRG is supported by a Ramón y Cajal research contract from the Spanish MICINN and co-financed by the European Social Fund.

#### References

- Asplund, M., Grevesse, N., Sauval, A. J., & Scott, P. 2009, *ARA&A*, 47, 481  
Draine, B. T. 1978, *ApJS*, 36, 595  
Gerin, M., Goicoechea, J. R., Pety, J., & Hily-Blant, P. 2009, *A&A*, 494, 977  
Goicoechea, J. R., Compiègne, M., & Habart, E. 2009a, *ApJ*, 699, L165  
Goicoechea, J. R., Pety, J., Gerin, M., Hily-Blant, P., & Le Boulrot, J. 2009b, *A&A*, 498, 771  
Goicoechea, J. R., Pety, J., Gerin, M., et al. 2006, *A&A*, 456, 565  
Habart, E., Abergel, A., Walmsley, C. M., Teyssier, D., & Pety, J. 2005, *A&A*, 437, 177  
Langer, W. D., Velusamy, T., Pineda, J. L., et al. 2010, *A&A*, 521, L17  
Le Boulrot, J., Le Petit, F., Pinto, C., Roueff, E., & Roy, F. 2012, *A&A*, 541, A76  
Le Petit, F., Nehmé, C., Le Boulrot, J., & Roueff, E. 2006, *ApJS*, 164, 506  
Müller, H. S. P., Thorwirth, S., Roth, D. A., & Winnewisser, G. 2001, *A&A*, 370, L49  
Neufeld, D. A., Schilke, P., Menten, K. M., et al. 2006, *A&A*, 454, L37  
Neufeld, D. A., Sonnentrucker, P., Phillips, T. G., et al. 2010, *A&A*, 518, L108  
Neufeld, D. A., Wolfire, M. G., & Schilke, P. 2005, *ApJ*, 628, 260  
Novotny, O., Mitchell, J. B. A., LeGarrec, J. L., et al. 2005, *Journal of Physics B Atomic Molecular Physics*, 38, 1471  
Penzias, A. A. & Burrus, C. A. 1973, *ARA&A*, 11, 51  
Pety, J. 2005, in *SF2A-2005: Semaine de l'Astrophysique Française*, ed. F. Casoli, T. Contini, J. M. Hameury, & L. Pagani, 721  
Pety, J., Goicoechea, J. R., Hily-Blant, P., Gerin, M., & Teyssier, D. 2007, *A&A*, 464, L41  
Pickett, H. M., Poynter, R. L., Cohen, E. A., et al. 1998, *J. Quant. Spec. Radiat. Transf.*, 60, 883  
Reid, R. V. & Chu, A. H.-M. 1974, *Phys. Rev. A*, 9, 609  
Snow, T. P., Destree, J. D., & Jensen, A. G. 2007, *ApJ*, 655, 285  
Sonnentrucker, P., Neufeld, D. A., Phillips, T. G., et al. 2010, *A&A*, 521, L12  
van der Tak, F. F. S., Ossenkopf, V., Nagy, Z., et al. 2012, *A&A*, 537, L10